Free Radical Research, May 2007; 41(5): 591–601

informa
healthcare

4-HPR-mediated leukemia cell cytotoxicity is triggered by ceramide-induced mitochondrial oxidative stress and is regulated downstream by Bcl-2

MARIA-CELIA MORALES[1], GORKA PÉREZ-YARZA[1], NAIARA N. REMENTERÍA[1], MARÍA-DOLORES BOYANO[1], AINTZANE APRAIZ[1], ANTONIO GÓMEZ-MUÑOZ[2], ENCARNA PÉREZ-ANDRÉS[2], & AINTZANE ASUMENDI[1]

[1]*Department of Cell Biology and Histology, Faculty of Medicine and Dentistry, University of the Basque Country, Barrio Sarriena s/n, E-48940 Leioa, Bizkaia, Spain, and* [2]*Department of Biochemistry and Molecular Biology, Faculty of Science and Technology, University of the Basque Country, Barrio Sarriena s/n, E-48940 Leioa, Bizkaia, Spain*

Accepted by Professor Dr T. Grune

(Received 19 September 2006; in revised form 15 December 2006)

Abstract

We have previously reported that, in leukemia cells, the cytotoxicity of the anticancer agent *N*-(4-hydroxyphenyl)retinamide (4-HPR) is mediated by mitochondria-derived reactive oxygen species (ROS) and cardiolipin peroxidation. Here, we have analyzed at greater depth the 4-HPR-triggered molecular events, demonstrating that 4-HPR induces an early (15 min) increase in ceramide levels by sphingomyelin hydrolysis and later (from 1 h) by *de novo* synthesis. Using specific inhibitors of both pathways, we demonstrate that ceramide accumulation is responsible for early ROS generation, which act as apoptotic signalling intermediates leading to conformational activation of Bak and Bax, loss of mitochondrial membrane potential ($\Delta\Psi m$), mitochondrial membrane permeabilization (MMP) and cell death. Enforced expression of Bcl-2 has no effect on 4-HPR-induced oxidative stress, but notably prevents mitochondrial alterations and apoptosis, indicating that Bcl-2 functions by regulating events downstream of ROS generation. In conclusion, our study delineates for the fist time the sequence and timing of the principal events induced by 4-HPR in leukemia cells and points to the potential use of modulators of ceramide metabolism as enhancers in 4-HPR-based therapies.

Keywords: *4-HPR, fenretinide, ROS, apoptosis, ceramide, Bcl-2*

Abbreviations: *4-HPR,* N-*(4-hydroxyphenyl)retinamide; ROS, reactive oxygen species; MMP, mitochondrial membrane permeabilization; SMase, sphingomielinase; AIF, apoptosis inducing factor; OMM, outer mitochondrial membrane; IMM, inner mitochondrial membrane*

Introduction

N-(4-hydroxyphenyl)retinamide (4-HPR), also known as fenretinide, is a synthetic derivative of all-trans-retinoic acid (ATRA), which has potent chemopreventive and anti-neoplasic properties [1]. The anticancer activity of 4-HPR seems to be related to its ability to inhibit tumour cell growth and to induce apoptosis [2–5]. In several tumor cell lines, 4-HPR induces apoptosis by a mechanism involving oxidative stress [3–6], but reactive oxygen species (ROS)-independent mechanisms have also been described [3]. Our group and others have identified the mitochondrial electron transport chain as the main

Correspondence: A. Asumendi, Department of Cell Biology and Histology, Faculty of Medicine and Dentistry, University of The Basque Country, E-48940 Leioa, Vizcaya, Spain. Tel: 34 94 601 5708. Fax: 34 94 601 3266. E-mail: aintzane.asumendi@ehu.es

ISSN 1071-5762 print/ISSN 1029-2470 online © 2007 Informa UK Ltd.
DOI: 10.1080/10715760701218558

source of 4-HPR-generated oxidative stress [7,8]. In addition, 12-lipoxygenase was recently reported to be activated by 4-HPR to produce ROS in neuroblastoma cells [9].

In recent years, two major pathways for the induction of extrinsic (death receptor-mediated) and intrinsic (mitochondrial) apoptosis have been identified [10]. Mitochondria play a major role in the intrinsic pathway which functions as the target of numerous pro-apoptotic signal mediators, such as sphingolipids, Ca^{2+}, ROS, etc. Within mitochondria, a variety of apoptosis-associated events also take place including changes in electron transport, altered mitochondrial oxidation–reduction, loss of mitochondrial membrane potential ($\Delta\Psi m$) and release of cytochrome *c*, apoptosis-inducing factor (AIF), smac-DIABLO, etc. [10]. The liberation of such apoptogenic molecules and the induction of downstream caspase activity is dependent on mitochondrial membrane permeabilization (MMP), which is controlled by several proteins of the Bcl-2 family, including Bax and Bak [11]. These proapoptotic proteins can undergo a conformational change which accompanies their apoptotic activation [12,13], consisting in the exposure of the N-termini, which are normally buried within the α-helical bundles of Bax and Bak [14].

Ceramide, a sphingosine-based lipid molecule, is suggested to have a central role in several cell-death pathways [15]. Within cells, ceramide can be generated as a result of sphingomyelin hydrolysis by sphingomyelinases (SMase) via a hydrolytic pathway or by a *de novo* biosynthetic pathway. A number of chemotherapeutic agents trigger the activation of SMase or *de novo* biosynthesis and generate ceramide, which acts as a cell death or growth inhibition mediator [16]. In addition, recent studies are beginning to clearly show that modulation of endogenous ceramide levels can modulate drug-mediated apoptosis [17–19]. A growing body of evidence indicates that ceramide generation and oxidative stress are intimately connected in cell death signalling. ROS have been implicated in the generation of ceramide and in the induction of apoptosis by ceramide [6,20,21]. In other studies ceramide was reported to induce apoptosis by increasing ROS generation or by inhibiting the ROS scavenger glutathione [15,22–24].

In this study, we have examined the nature and relevance of ceramide production and signalling in response to exposure of leukemia cells to 4-HPR and its relationship to mitochondria-derived oxidative stress. The data presented here contribute to a better understanding of the apoptotic pathway triggered by the antineoplasic agent in leukemia cells, demonstrating that ceramide levels are increased by 4-HPR to produce ROS, which ultimately act as apoptotic signalling intermediates, mediating Bcl-2-regulated mitochondrial alterations.

Materials and methods

Cell lines and culture conditions

CCRF-CEM human acute lymphoblastoid leukemia cells were grown in RPMI 1640 (Life Technologies) supplemented with 10% heat inactivated fetal bovine serum, 100 μg/ml gentamycin and 2 mM L-glutamine. 10E1-CEM cells were CCRF-CEM cells transfected with a Bcl-2 cDNA-containing vector overexpressing Bcl-2 [25], kindly provided by Dr Kofler. The density of cultured cells for assay was 10^6 cell/ml.

CCRF-CEM cells were treated with 50 μM desipramine for 2 h (sphingomyelinase inhibitor, Sigma Chemical Co.) and 1.5 μM GT11 for 72 h (specific dihydroceramide desaturase inhibitor [26]), kindly provided by Dra. Fabriàs. In other experiments, 100 μM vitamin E (Sigma) or 100 μM z-VAD-fmk (Bachem) was added to cells 2 h before drug application.

Cell survival assay

A standard XTT assay (Roche Molecular Biochemicals, IN, USA) was used to determine cell survival. Cells were plated in 96-well plates at a density of 10^6 cells/ml (four wells per experimental condition), exposed to a range of concentrations of 4-HPR and processed according to the manufacturer's instructions. Absorbance at 480 nm was determined for each well and cell survival percentages were calculated in each experiment in relation to control (non-4HPR) treated cells.

Immunofluorescence and microscopy

After 4-HPR treatment, cells were layered on coverslips pretreated with poly-L-lysine 0.001% (Sigma). They were then fixed with paraformaldehyde (4% w/v) and their membranes were permeabilized (0.1% SDS) for immunofluorescence assays. Cells were stained for the detection of activated Bak (mAb Ab-1, Oncogene) and activated Bax (mAb 6A7, Pharmingen). The presence of these primary antibodies was detected using anti-mouse-IgG secondary antibodies conjugated to FITC (Sigma). Cell nuclei were counterstained with DAPI (Molecular Probes) before mounting. Digital images were obtained with a fluorescent microscope (Axioskop 2, Zeiss, Germany) connected to a digital camera (Coolsnap photometrycs).

Western blotting

Cell pellets were resuspended at 4°C in 300 μl HNB buffer (10 mM PIPES, 2 mM $MgCl_2$, 10 mM KCl pH 7.4), supplemented with 1 mM DTT, 0.1 mM PMSF, 20 μM cytocalasin B and a protease inhibitor cocktail (Roche). The cells were then disrupted by homogenization on ice by a douncer (150 strokes) and the

homogenate was subjected to 30% sucrose gradient. After centrifugation at 1200*g* for 15 min the supernatant was collected and subjected to centrifugation at 10,000*g* for 30 min at 4°C. The mitochondrial pellet was removed and the supernatant was subjected to another centrifugation at 46,000*g* for 1 h to obtain cytosolic extract. Total protein content was determined with the Bio-RAD DC kit. Samples of the cytosolic extracts containing 20 μg protein were loaded into a 12% SDS-polyacrylamide gel, transferred to nitrocellulose membranes and subjected to immunodetection of AIF (Chemicon). The binding of the antibody was detected using the ECL chemiluminescence method (Pierce Supersignal®).

Flow cytometry

Propidium iodide (PI) (50 μg/ml) was used to determinate cell hypoploidy and DCFH-DA (10 μg/ml) was employed for the determination ROS overproduction. Reduction of $\Delta\Psi m$ was evaluated by incubating cells with 100 nM $DiOC_6(3)$. All of these fluorochromes were purchased from Molecular Probes. After incubating with fluorochromes, cells were washed and analyzed by flow cytometry. At least 10,000 viable cells per sample were individually analyzed for quantitative fluorescence using a Coulter EPICS ELITE ESP flow cytometer (EPICS division Coulter Corp.).

Measurement of intracellular generation of ROS by cytofluorimetry

We used DCFH-DA (Molecular Probes, Eugene, OR) to measure the production of ROS. Cells seeded in 96 well culture plates at a density of 10^6 cells/ml (four wells per experimental condition) were exposed to different concentrations of 4-HPR for 30 min. About 10 μg/ml DCFH-DA was added 20 min before treatment had finished. After washing, fluorescence intensity was measured at 530 nm after excitation at 485 nm in a Fluoroskan Ascent fluorimeter (Labsystems).

DAG assay for determination of ceramide levels

CCRF-CEM cells were seeded at 10^6 cells/ml, rested overnight and then treated with 6 μM 4-HPR. Lipids were collected according to the method of Bligh and Dyer [27]. In brief, cells were pelleted, washed once with PBS and then extracted with 1 ml methanol. The monophase was mixed and the organic and aqueous phases were subsequently separated by the addition of 1 ml chloroform and 0.9 ml water followed by vigorous shaking and centrifugation at 300*g*. The aqueous phase was carefully aspirated and the organic phase washed twice with 1 ml 2 M KCl/0.2 M HCl. Aliquots of the organic phase were transferred to new tubes and dried down for ceramide and phosphate measurements. Ceramide levels were determinated using the diacylglycerol kinase assay [28]. The reaction buffer was prepared as a solution containing 50 mM imidazole HCL pH = 6.6, 50 mM NaCl, 12.5 mM $MgCl_2$, 1 mM EGTA, 1.2 mM DETAPAC, 1 mM cardiolipin, 10 mM dithiothreitol, 1.5% (w/v) *N*-octyl-β-D-glucopyranoside, 1 mM ATP, 5 μg/assay 1,2-diacylglycerol kinase from *E. Coli* (Sigma) and 1 μCi/assay [γ-32P]ATP solution (specific activity of 3000 cpm/mmol). The reaction was started by solubilizing the dried lipid in 100 μl of the previous solution. Samples were incubated for 90 min at 37°C, then the reaction was stopped by adding 1 ml methanol. Lipids were again extracted as described above and an aliquot of the organic phase was vacuum-dried. Lipids were then resuspended in a volume of 50 μl chloroform and spotted onto a 20 cm silica gel thin layer chromatography plate (TLC). The TLC plates were developed with chloroform/methanol/ammonium hydroxide (65:35:7.5 v/v/v), air dried and then redeveloped with chloroform/acetone/methanol/acetic acid/H_2O (50:20:10:10:5 v/v/v/v/v). After autoradiography, the radioactive spots corresponding to ceramide phosphate (the phosphorylated product of ceramide), were scraped into a scintillation vial containing 4 ml scintillation fluid and counted using a scintillation counter. Linear curves of phosphorylation were produced over a concentration range of 0–4 nmol of external ceramide standards (Sigma Chemical Co., St Louis, MO). Ceramide levels were always normalized to lipid phosphate.

Lipid phosphate determination

Lipid phosphate was measured by acid hydrolysis. The chloroform phase of the extract was evaporated and the lipids were incubated at 180°C for 30 min in 50 μl of 60% $HClO_4$. After acid hydrolysis, 278 μl of H_2O, 55 μl of 2.5% (w/v) ammonium molybdate and 55 μl of 10% ascorbic acid were added and incubated for 15 min in boiling water. Inorganic phosphate was detected by measuring absorbance at 700 nm and quantified based upon a standard curve of glycerol-3-phosphate.

^{3}[H] myristate assay for determination of ceramide levels

CCFR-CEM cells (10^6 cells/ml) were labeled overnight with 3 μCi/ml of [^{3}H]myristate (NEM-Boston, MA). The radioactive medium was then removed by centrifugation and the cells washed three times with isotonic saline solution and resuspended in RPMI medium and treated with 6 μM 4-HPR. Lipids were extracted as described by Bligh and Dyer [31], except that 2 M KCl in 0.2 M HCl was added to the extraction mixture instead of water for separation of phases. Chloroform phases were then vacuum-dried in an

automatic Speed Vac concentrator (Savant AS290) and resuspended in 50 μl chloroform. Lipids were separated by TLC using 20 cm silica gel 60-coated aluminum plates. TLC plates were developed for 50% of their lengths with chloroform/methanol/acetic acid (9:1:1, v/v/v) and then dried. The plates were then redeveloped for their full lengths with petroleum ether/diethylether/-acetic acid (60:40:1, v/v/v). The position of the lipids was identified after staining with I_2 vapor by comparison with authentic standards. [^{3}H]ceramides in the silica gel were quantified by liquid scintillation counting after scraping from the plates. Ceramide radioactivity was normalized to total lipid dpm.

Statistics

Results were expressed as the mean ± SD of at least three independent experiments. The Student two-tailed, unpaired *t*-test was used and values of $p < 0.05$ were considered to be significant.

Results and discussion

Early ROS generation by 4-HPR activates the intrinsic apoptotic pathway in CEM leukemia cells

We have previously demonstrated that 4-HPR induces mitochondria-derived oxidative stress in leukemia cells. Here, our purpose was to characterize temporarily and connect such oxidative stress with events involved in the apoptotic pathway. The T-cell acute lymphoblastic leukemia line CCRF-CEM was exposed to 4-HPR and ROS generation was determined after labelling with DCFH-DA, either by flow cytometry (Figure 1(A)) or plate fluorimetry (Figure 1(B)). 4-HPR was found to induce intense oxidative stress in CEM cells, as has been reported for other tumor lines [2,8]. Thus, after 30 min treatment, all cells presented elevated levels of ROS production (Figure 1(A)) which were somewhat lower than those associated with H_2O_2 (positive control). Kinetic studies (Figure 1(B)) demonstrated significant ROS generation as early as 15 min after drug exposure. ROS generation was time- and dose-dependent and rose to almost 4-fold that of control levels at 10 μM 4-HPR.

Monoclonal antibodies were used to detect the activation of the proapoptotic proteins Bak and Bax as previously described (Ab-1 for Bak and 6A7 for Bax; [29]). We observed that while untreated CEM cells exhibited no staining with either the Bak (Figure 1(C)) or Bax-specific antibodies, 4-HPR-treated cells exhibited a bright, punctate cytoplasmic staining pattern, consistent with the conformational activation of Bax/Bak, which was perceptible after 4 h of 4-HPR-treatment. Vitamin E inhibited this activation (Figure 1(D)), indicating that in leukemia cells, Bak and Bax were activated in response to 4-HPR mediated oxidative stress, as has been reported to occur in cervical carcinoma cells [29] and neuroblastoma cells [30].

Loss of $\Delta\psi m$ was determined by assessing the incorporation of the $\Delta\psi m$-sensitive dye $DIOC_6(3)$ [31]. Kinetic analysis showed that 4-HPR induced an early dissipation of $\Delta\psi m$ in a concentration- and time-dependent manner (Figure 1(E)). 4-HPR induced the antioxidant-inhibitable release of AIF to the cytosol (Figure 1(G)), as well as cytocrome *c* [7], leading to nuclear apoptosis as indicated by the presence of hypodiploid cells (Figure 1(F)). Inhibition of caspase activation by addition of the pan-caspase inhibitor Z-VAD-fmk totally prevented nuclear apoptosis (Figure 1(F)) with little effect on $\Delta\psi m$ (data not shown) that could be explained as a caspase-mediated amplification of apoptosis signal.

All these data point to the activation of the ROS-mediated mitochondrial pathway in which the Bcl-2 family proteins Bax and Bak are implicated. We demonstrate for the first time that the ROS scavenger vitamin E efficiently inhibits changes in Bak/Bax conformation (Figure 1(D)), $\Delta\psi m$ (Figure 1(E)) and AIF localization (Figure 1(G)). Overall, this data indicates that ROS play an instrumental role in HPR-induced MMP, possibly mediating Bak and Bax activation (Figure 1(D)). Many apoptotic signals can trigger BH3-only-protein-dependent translocation of Bax, followed by its insertion into the outer mitochondrial membrane (OMM) [32] and the formation of Bak or Bax homo-oligomers [33], which are likely exit conduits in the OMM for proapoptotic proteins. Alternatively, H_2O_2—or its intracellular production during drug-induced apoptosis—can act as a direct signal for mitochondrial translocation of Bax, which is mediated by cytosolic acidification [34]. However, simple permeabilization of the OMM is not sufficient for cytochrome *c* release [35,36]. In this sense, ROS-mediated peroxidation of cardiolipin, which we have demonstrated to occur in leukemia cells after 4-HPR-treatment [7], could be a critical first step in order to mobilize cytochrome *c* from the inner mitochondrial membrane (IMM) [35,36]. Thus, 4-HPR-induced ROS can promote the two neccesary steps to release cytochrome *c*: disruption of the association of cit *c* with cardiolipin by its peroxidation [35,37] and release of the solubilized pool via permeabilization of the OMM by Bax and/or Bak. Our recent findings indicating that glutathione contents contribute to determining the sensitivity of different tumor lines to 4-HPR [31], reinforce the pivotal role of ROS in the 4-HPR-induced apoptotic pathway.

Upstream ceramide accumulation leads to ROS overproduction, loss of mitochondrial membrane potential and apoptosis in 4-HPR-treated leukemia cells

4-HPR has been reported to increase intracellular levels of ceramide in some tumor cells [38], but the link

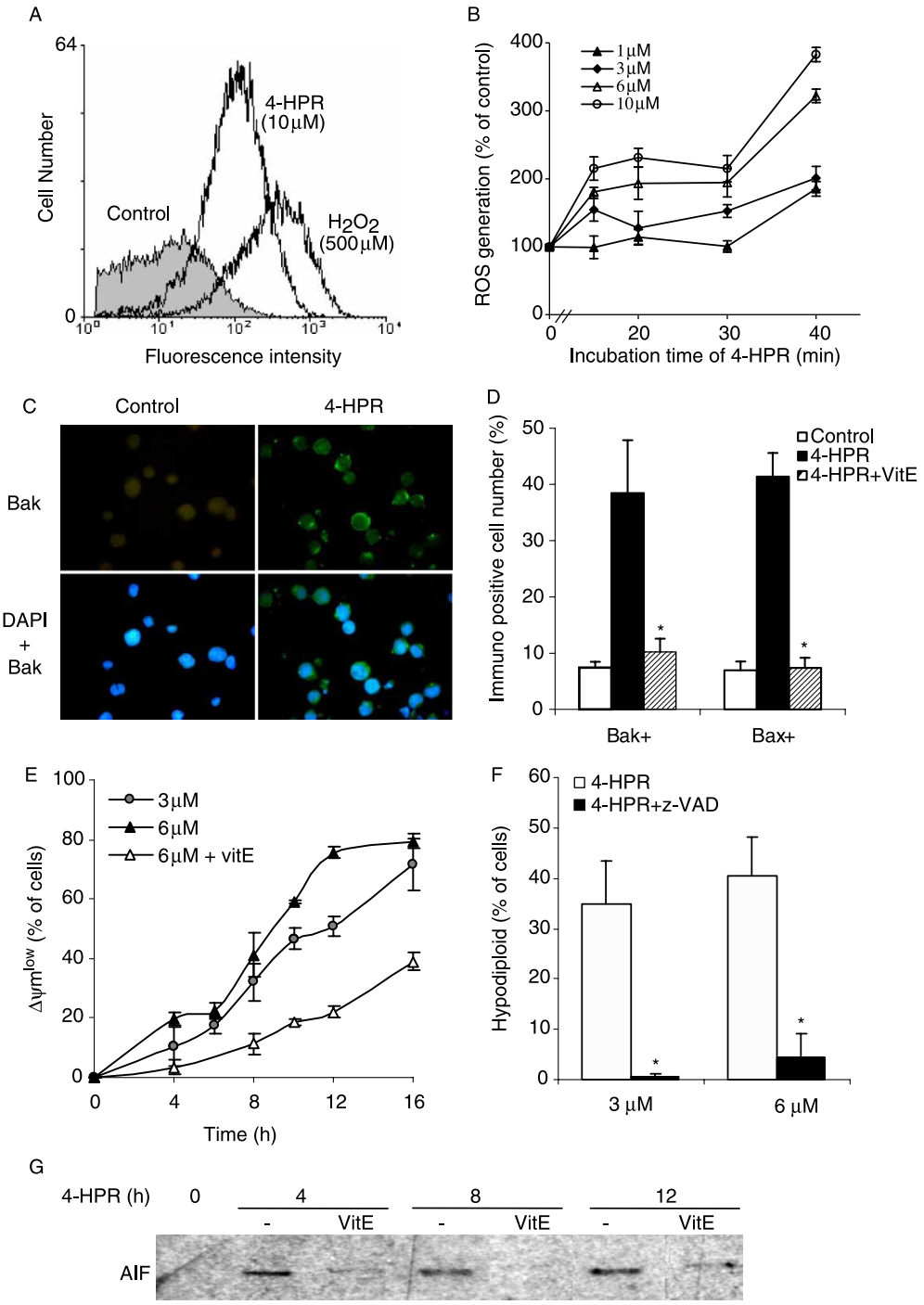

Figure 1. Early ROS generation by 4-HPR actives an intrinsic apoptotic pathway. (A) 4-HPR increases ROS levels in CCRF-CEM leukemia cells. ROS levels were assayed with DCFH-DA after 30 min 4-HPR incubation and H_2O_2 was used as a positive control. (B) Time and concentration course of 4-HPR-induced ROS overproduction in CCRF-CEM. Data are expressed as relative percentages of the fluorescence emitted by DCFH-DA with respect to non-treated control cells (100%). Means ± SD of three experiments are shown. (C) 4-HPR induces the activation of Bak and Bax. CCRF-CEM cells untreated or treated with 6 μM 4-HPR for 4 h were stained with DAPI together with antibodies specific for the N-terminus of Bak and Bax (the latter not shown) and representative microphotographs are shown. (D) Cells treated with 4-HPR in the presence and absence of vitamin E (100 μM) were also stained for the detection of active Baμk and Bax and the number of immunopositive cells was quantified. Results are expressed as the mean ± SD of three independent experiments; differences between 4HPR vs. 4HPR + vit E were found to be statistically significant ($\star p < 0.05$). (E) Dose- and time-dependent assay of MMP by 4-HPR. Cells were incubated with 3 and 6 μM 4-HPR for the indicated times and then stained with $DiOC_6(3)$, a ΔΨm-sensitive fluorochrome and analyzed by flow cytometry. Note that vitamin E (100 μM) was able to significantly reduce the fall in ΔΨm. Cells with low ΔΨm were < 4% in the controls. (F) Effect of the caspase inhibitor z-VAD-fmk on the induction of 4-HPR-mediated hypodiploidy. CCRF-CEM cells were incubated in the presence and absence of z-VAD-fmk (100 μM) for 1 h and then the cells were treated with 4-HPR for 12 h. Cells were stained with PI and hypodiploid cell number was detected by flow cytometry; values represent means ± SD of three independent experiments; differences between 4HPR vs. 4HPR + z-VAD-fmk were found to be statistically significant ($\star p < 0.05$). (G) 4-HPR induced mitochondrial AIF release.

between ceramide and subsequent apoptosis in leukemia cells is unclear. Since ROS production is an early event in 4HPR-induced toxicity in leukemia cells (Figure 1(A) and (B)), we studied the relationship between ceramide generation and ROS overproduction, analyzing both processes at early times. First, cells were treated with 4-HPR and total ceramide levels (A) and ceramides derived from sphygomyelin hydrolysis (B) were measured over 4 h. As shown in Figure 2, 4-HPR leads to a biphasic increase in the levels of intracellular ceramide (Figure 2(A)): an early peak was observed after 15 min and a later peak was detected 2 h after treatment. Only the early peak was observed when measuring ceramide derived from sphingomyelin hydrolysis (Figure 2(B)), indicating that that second peak was likely caused by *de novo* ceramide synthesis. This data indicates that the 4-HPR-mediated increase in ceramide levels has a dual origin and that this increase is an early event, preceeding apoptosis-associated mitochondrial alterations, which take place at least 4 h after drug exposure (Figure 1). To the best of our knowleage, the kinetics of 4HPR-induced early ceramide generation in leukemia cells has not been characterized up to now.

In order to investigate the sequence of events in the 4-HPR triggered signalling pathway, CEM cells were incubated with either desipramine or GT11 before they were incubated with 4-HPR and then ROS generation were measured. Desipramine is a specific inhibitor of neutral sphingomyelinase and GT11 is the first, novel specific inhibitor of dihydroceramide desaturase, the enzyme involved in the last step of the *de novo* biosynthetic pathway of ceramide [26]. Because dihydroceramide is usually much less effective or fails to show the bioactivity of ceramide, this step seems to be of particular importance. Both inhibitors had consequences on 4-HPR-mediated ROS generation (Figure 3). Desipramine blocked early ROS generation but was unable to suppress late ROS generation (Figure 3(A)). In contrast, GT11 did not affect the early phase of ROS overproduction but effectively inhibited ROS generated after 60 min (Figure 3(B)). No ROS overproduction was observed when ROS generation was measured in the presence of both inhibitors (data not shown). These results corroborate the activation by 4-HPR of both ceramide synthesis pathways and demonstrate that ceramide accumulation occurs upstream of oxidative stress generation. GT11 further suppressed the loss of $\Delta\psi m$ (Figure 4(A)) and notably reduced 4-HPR-induced cell death (Figure 4(B)), pointing to ROS generated by *de novo*-synthesized ceramide as the main factor responsible for mitochondrial dysfunction, membrane permeabilization and apoptosis. However, the relative importance of each ceramide synthesis pathway in 4-HPR-triggered apoptotic signalling could not be determined, since the same studies with desipramine could not be repeated over medium and long time scales due to its high toxicity.

It is known that several retinoid derivatives act directly on isolated mitochondria [39,40]. However, in HeLa cells, 4-HPR does not induce MMP through a direct action on mitochondria or on the mitochondrial permeability transition pore complex (PTPC) [29]. Thus, the ability of 4-HPR to generate ROS (Figure 1(A) and (B)), mitochondrial despolarization (Figure 1(E)) and permeabilization (Figure 1(G)), must involve mediators generated outside of mitochondria. The findings presented in this work provide strong evidence that ceramide acts as the intracellular mediator of ROS generation in the apoptotic pathway triggered by 4-HPR in leukemia cells. Even if the role of ceramide in cell death is well documented, the mechanism by which ceramide elicits apoptosis has not been fully elucidated and the pathways seem to be both stimulus- and cell-type specific. In the most cases, ROS appears to induce ceramide synthesis mainly via SMase activation [15], but emerging evidence indicates that mitochondria appear to be targets for ceramide itself [41]. Several authors have reported how ceramide is able to act directly on the mitochondrial respiratory complex generating ROS [42–45], a decrease in mitochondrial transmembrane potential [22,46] and release of both cytocrome *c* [44,46,47] and AIF [47]. In any case, ceramide has been shown to be both a signalling product of oxidative stress and a mediator of the production of reactive oxidants in mitochondria [15,42,43,45]. Our findings point to the latter role since we have demonstrated elsewhere the mitochondrial origin of 4-HPR-induced ROS, at a target between the mitochondrial respiratory chain complexes II and III [7].

Several studies have identified the mitochondrial ubiquinone pool of complex III as a ceramide target to produce ROS [42,43,45]. Interestingly, complex III is also affected by molecules which trigger ceramide production in their apoptotic signalling, such as TNF-α [48] or anticancer drugs [49,50], suggesting that mitochondria and in particular the respiratory electron chain, behave as a target for ceramide. Maurer et al. [17] have demostrated a synergistic cytotoxicity between 4-HPR and modulators of ceramide metabolism in neuroblastoma cells. Our findings also point to the same

Cells were incubated at the times indicated with 6 μM 4-HPR with or without vitamin E (100 μM), followed by recovery of cytosol protein extracts and detection of cytosolic AIF by immunoblot. Equal protein loading was verified by Ponceau red staining before transfer to nitrocellulose membranes.

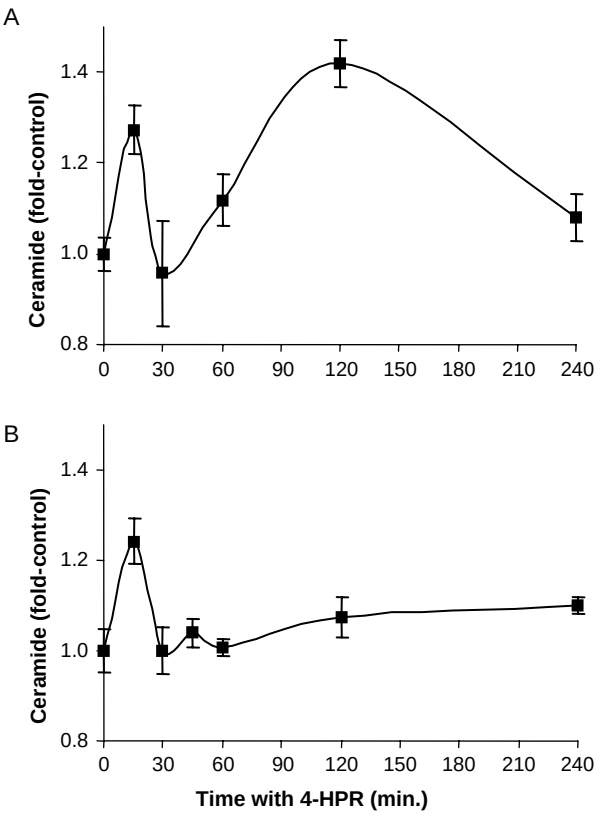

Figure 2. 4-HPR induced a rapid increase of sphingomyelin hydrolysis and a later *de novo* ceramide synthesis. Kinetics of (A) total ceramide and (B) ceramide from sphingomyelin hydrolysis, in CCRF-CEM cells expose to 6 μM 4-HPR. (A) Ceramide mass measurements were determined using the diacylglycerol kinase assay and [γ-^{32}P]ATP, after lipid extraction. (B) To determine ceramide derived from sphingomyelin hydrolysis, cells were labeled overnight with [^{3}H]myristate, before 4-HPR treatment. Values represent the mean ± SD of three independent experiments and were calculated as a percentage of those measured in control cells, not exposed to 4-HPR.

possibility in leukemia cells and we are currently conducting experiments to elucidate this issue. However, the mechanisms of generating oxidative stress do not appear to be the same in both cases; whilst in leukemia cells ceramide accumulation induced ROS at a mitochondrial level [7], in neuroblastoma cells, gangliosides derived from ceramide metabolism lead to the induction of ROS via 12-lipoxygenase [9]. Also, the generation of ceramide appears to be different in both cases: in neuroblastoma cells, ceramide derived exclusively from sphingomyelin, but in CEM cells both pathways become activated even though *de novo* synthesis seems to have a predominant function in mitochondrial damage and apoptosis (Figures 2–4).

Bcl-2 regulates ROS-mediated mitochondrial apoptotic events in 4-HPR-treated cells but not ROS production

The anti-apoptotic protein Bcl-2, mainly located in mitochondria, is thought to function by regulating MMP [11]. Because 4-HPR activates the pro-apoptotic proteins Bak and Bax and mitochondria seem to integrate 4-HPR triggered signalling (Figure 1), we employed stably Bcl-2-transfected CEM cells (E1) to investigate the role of this protein in the 4-HPR-activated apoptotic pathway. Overexpression of Bcl-2 provided significant protection from the apoptotic effects of 4-HPR (Figure 5(A)). About 1 μM 4-HPR scarcely affected cell viability and cell death decreased from near 80% in native cells to 20% in transfected ones at a dose of 3 μM. However, in E1 cells, 4-HPR-induced oxidative stress was not prevented (Figure 5(B)), indicating that the protection exerted by Bcl-2 occurs downstream of ceramide-mediated ROS production. Whereas native cells manifested a progressive dissipation of $\Delta\psi m$ when exposed to 4-HPR, Bcl-2-transfected cells conserved an almost normal $\Delta\psi m$, even after 12 h of treatment (Figure 5(C)). In native cells, dissipation of $\Delta\psi m$ is clearly associated with apoptosis since $DiOC_6(3)$ labelling decreased without membrane permeabilization (PI) (Figure 5(C)), marking the point of no return.

Measurement of cytosolic Ca^{2+} levels during treatment demonstrated that 4-HPR increased its concentration after 8 h with respect to control basal

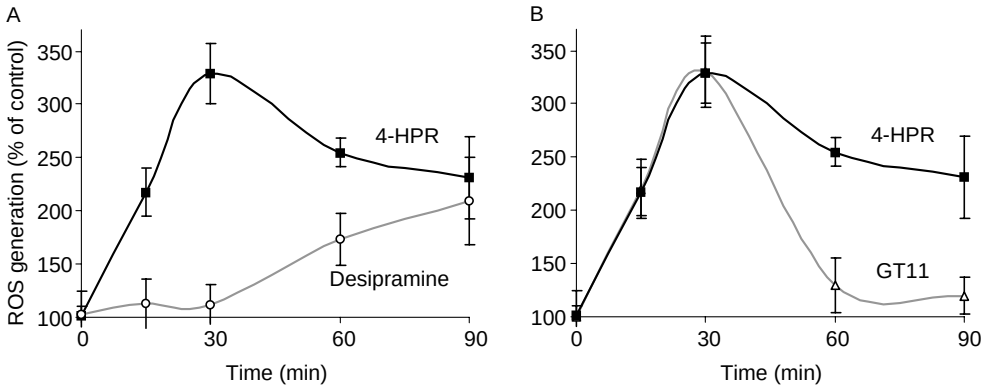

Figure 3. Ceramide synthesis induces ROS overproduction. Kinetic study of 4-HPR-induced ROS overproduction in the presence of ceramide synthesis inhibitors. CCRF-CEM cells were incubated with (A) 50 μM desipramine for 2 h or (B) 1.5 μM GT11 for 72 h, followed by 6 μM 4-HPR for the indicated times. ROS production was measured by cytofluorimetry using DCFH-DA. Relative values with respect to non-treated CCRF-CEM cells (100%) are shown. Values represent the mean ± SD of three independent experiments.

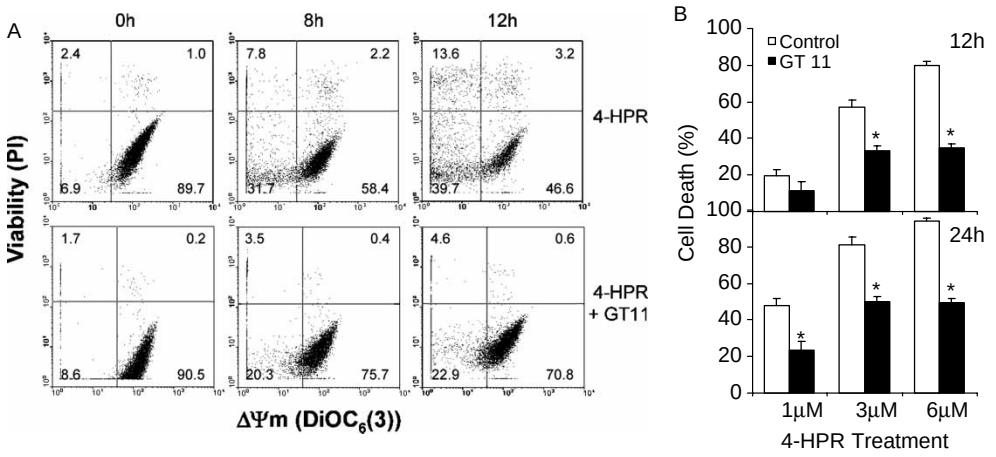

Figure 4. Inhibition of *de novo* ceramide synthesis protects against the loss of ΔΨm and cell death induced by 4-HPR in CCRF-CEM cells. Cells were cultured in the presence or absence of GT11 (1.5 μM, 72 h) and subsequently exposed to 4-HPR for the indicated times. (A) 3 μM 4-HPR-treated cells were stained with $DiOC_6(3)$ and PI to determine the percentage of cells with low ΔΨm and viability, respectively. Numbers in quadrants refer to the percentage of cells. Pictograms representative of three independent experiments are shown. (B) The percentage of cell death was determined by colorimetric assay after 12 and 24 h of 4-HPR treatment. Relative percentages with respect to untreated cells are shown. The means ± SD of three experiments are shown; differences between GT11 vs. control were found to be statistically significant ($\star p < 0.05$).

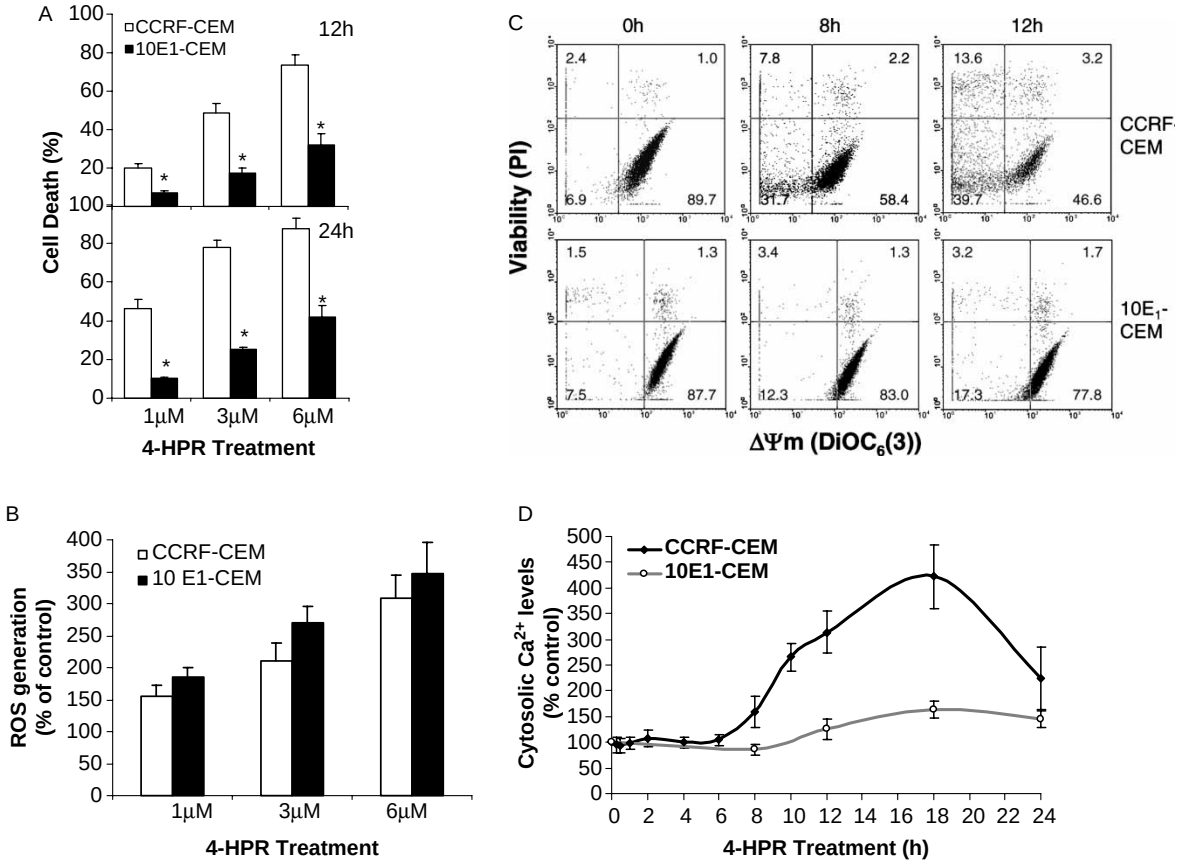

Figure 5. Bcl-2 regulates ROS-mediated mitochondrial apoptotic events. Comparative assays of 4-HPR-treatment effects on CCRF-CEM and $10E_1$-CEM cells. (A) Cell death was determined by a colorimetric assay at the indicated doses and time. In all cases, values with respect to non-treated, control cells represent the mean ± SD of three independent experiments, each performed in quadruplicate; differences between CCRF-CEM vs. 10E1-CEM were found to be statistically significant ($\star p < 0.05$). (B) Cells were treated with 4-HPR at the indicated doses for 30 min and stained with the ROS-sensitive dye DCFH-DA. (C) Cells were incubated with 3 μM 4-HPR for the indicated times and then stained with $DiOC_6(3)$/PI, followed by flow cytometry evaluation. The percentage of cells with a low ΔΨm was higher in CCRF-CEM cells than in $10E_1$-CEM cells. Dot plots are representative of four independent experiments; numbers in quadrants indicate percentages of cells. (D) Kinetic study of cytosolic Ca^{2+} levels after 6 μM 4-HPR treatment. Cytosolic Ca^{2+} was determined using Fluo-4, as described in the Materials and Methods section.

concentrations; after 12 h, treated cells showed a 3-fold increase in cytosolic Ca^{2+} and reach a maximum at 18 h (Figure 5(D)). Ca^{2+} increments could be, in some cases, a consequence of the inhibition of reticulum-ATPase [51]. However, 4-HPR-mediated elevation of cytosolic Ca^{2+} occurs downstream Bak/Bax activation, loss of $\Delta\psi m$ and AIF release (Figure 1). Thus, it appears to be a consequence of MMP rather than its cause [52]. Consistently, Bcl-2 overexpression also inhibited the liberation of Ca^{2+} to the cytosol in E1 cells (Figure 5(D)).

The fact that Bcl-2 overexpression inhibited mitochondrial apoptosis even in the presence of high amounts of ROS, indicates that it regulates crucial downstream events acting before the point-of-no-return. Because the interplay of different clases of Bcl-2 family proteins is crucial in determining the ultimate mitochondrial response [11], Bcl-2 can exert its protective function in different manners. For instance, Bcl-2 may form inactivating heterodimers with Bak/Bax [53], but may also sequester active BH3-only proteins [54]. Bax and Bak can also cooperate with the mitochondrial permeability transition pore (PTP) to form a channel in the OMM and Bcl-2 can inhibit this [10].

Concluding remarks

The data presented in this paper indicate that the first signal in the 4-HPR-triggered apoptotic pathway is the accumulation of ceramide (Figure 2), which is derived from both early sphingomyelinase hydrolisis (15 min) and a later *de novo* synthesis (2 h). Based on our previous work [7], we propose that 4-HPR-induced ceramide can act directly on mitochondria, inducing an oxidative stress which activates the intrinsic apoptotic pathway (Figure 1), a process which is tightly regulated by Bcl-2-family proteins (Figures 1(C) and (D) and 5). Many data argue in favor of such a hypothesis: (a) ceramide might be an early essential death signaling intermediate—mainly *de novo* synthetized ceramide—since avoiding its accumulation—by the use of specific inhibitors—we can abrogate the corresponding oxidative stress (Figure 3) and notably inhibit the loss of $\Delta\psi m$ (Figure 4(A)) and apoptotic cell death (Figure 4(B)). (b) ROS have an instrumental role because they are the ultimate factors which are responsible for Bak/Bax activation, mitochondrial membrane despolarization, MMP and activation of apoptotic caspases (Figure 1). (c) Transfection-enforced overexpression of Bcl-2 inhibits the dissipation of $\Delta\psi m$ and cell death, but not oxidative stress, thus indicating the importance of Bcl-2-regulating downstream apoptotic events in mitochondria. The identification of ceramide as an early mediator of the 4-HPR-triggered apoptotic signal raises the possibility that combining 4-HPR and modulators of ceramide metabolism may represent a novel antileukemic strategy, similar to that referred to by Maurer et al. in solid tumor lines [17].

Acknowledgements

We would like to thank Dr A. Fabrias for kindly providing GT11 and Dr A. Alvarez-Díaz for her assistance with flow cytometry. The English of this paper has been corrected by the agency ACTS (http://www.euskalnet.net/acts). This work was supported by grants from the University of the Basque Country (UPV 77.125-E-15360/2003 and UPV 75.327-14466/2002) and the Instituto de Salud Carlos III (FIS CO3/10, Nodo 11). Naiara Rementería holds a scholarship from the University of the Basque Country UPV/EHU and Aintzane Apraiz received a fellowship from the Spanish Ministery of Education and Culture.

References

[1] Fontana A, Rishi AK. Classical and novel retinoids: Their targets in cancer therapy. Leukemia 2002;16:463–472.
[2] Maurer BJ, Metelitsa LS, Seeger RC, Cabot MC, Reynolds CP. Increase of ceramide and induction of mixed apoptosis/necrosis by *N*-(4-hydroxyphenyl)-retinamide in neuroblastoma cell lines. J Natl Cancer Inst 1999;91:1138–1146.
[3] Sun SY, Li W, Yue P, Lippman SM, Hong WK, Lotan R. Mediation of *N*-(4-hydroxyphenyl)retinamide-induced apoptosis in human cancer cells by different mechanisms. Cancer Res 1999;59:2493–2498.
[4] Tosetti F, Vene R, Arena G, Morini M, Minghelli S, Noonan DM, Albin A. *N*-(4-hydroxyphenyl)retinamide inhibits retinoblastoma growth through oxygen species-mediated cell death. Mol Pharmacol 2003;63:565–573.
[5] Darwiche N, Hatoum A, Dbaibo G, Kadara H, Nars R, AbouLteif G, Bazzi R, Hermine O, de The H, Bazarbachi A. *N*-(4-hydroxyphenyl)retinamide induces growth arrest and apoptosis in transformed cell. Leukemia 2004;18:607–615.
[6] Rehman F, Shanmugasundaram P, Schrey MP. Fenretinide stimulates redox-sensitive ceramide production in breast cancer cells: Potential role in drug-induced cytotoxicity. Br J Cancer 2004;91:1821–1828.
[7] Asumendi A, Morales MC, Alvarez A, Aréchaga J, Pérez-Yarza G. Implication of mitochondria-derived ROS and cardiolipin peroxidation in *N*-(4-hydroxyphenyl)retinamide-induced apoptosis. Br J Cancer 2002;86:1951–1956.
[8] Suzuki S, Higuchi M, Proske RJ, Oridate N, Hong WK, Lotan R. Implication of mitochondrial-derived reactive oxygen species, cytochrome *c* and caspase-3 in *N*-(4-hydroxyphenyl)-retinamide-induced apoptosis in cervical carcinoma cells. Oncogene 1999;18:1951–1956.
[9] Lovat PE, Di Sano F, Corazzari M, Fazi B, Donnorso RP, Pearson ADJ, Hall AG, Redfern CPF, Piacentini M. Gangliosides link the acidic sphingomyelinase-mediated induction of ceramide to 12-lipoxygenase-dependent apoptosis of neuroblastoma in response to fenretinide. J Natl Cancer Inst 2004;96:1288–1299.
[10] Kroemer G, Reed JC. Mitochondrial control of cell death. Nat Med 2000;6:513–519.
[11] Breckenridge D, Xue D. Regulation of mitochondrial membrane permeabilization by BCL-2 family proteins and caspases. Curr Opin Cell Biol 2004;16:647–652.
[12] Korsmeyer SJ, Wei MC, Saito M, Weiler S, Oh KJ, Schelesinger PH. Proapoptotic cascade activates BID, which

oligomerizes BAK or BAX into pores that result in the release of cytochrome *c*. Cell Death Differ 2000;7:1166–1173.

[13] Letai A, Bassik MC, Walensky LD, Sorcinelli MD, Weiler S, Korsmeyer SJ. Distinct BH3 domains either sensitize or activate mitochondrial apoptosis, serving as prototype cancer therapeutics. Cancer Cell 2002;2:183–192.

[14] Suzuki M, Youle RJ, Tjandra N. Structure of Bax: Coregulation of dimer formation and intracellular localization. Cell 2000;103:645–654.

[15] Andrieu-Abadie N, Gouazé V, Salvayre R, Levade T. Ceramide in apoptosis signaling: Relatioship with oxidative stress. Free Radic Biol Med 2001;31:717–728.

[16] Modrak DE, Gold DV, Goldenberg DM. Sphingolipid targets in cancer therapy. Mol Cancer Ther 2006;5:200–2008.

[17] Maurer BJ, Melton L, Billups C, Cabot MC, Reynolds CP. Synergistic cytotoxicity in solid tumor cell lines between *N*-(4-hidroxyphenyl)retinamide and modulators of ceramide metabolism. J Natl Cancer Inst 2000;92:1897–1909.

[18] Batra S, Reynolds P, Maurer BJ. Fenretinide cytotoxicity for Ewing's sarcoma and primitive neuroectodermal tumor cell lines is decreased by hypoxia and synergistically enhanced by ceramide modulators. Cancer Res 2004;64:5415–5424.

[19] Litvak DA, Bilchik AJ, Cabot MC. Modulators of ceramide metabolism sensitize colorectal cancer cells to chemotherapy: A novel treatment strategy. J Gastrointest Surg 2003;7:140–148.

[20] Mansat-de Mas V, Bezombes C, Quillet-Mary A, Bettaieb A, D'Orgeix AD, Laurent G, Jeffrezou JP. Implication of radical oxygen species in ceramide generation, c-Jun N-terminal kinase activation and apoptosis induced by daunorubicin. Mol Pharmacol 1999;56:867–874.

[21] Cabrero A, Algret M, Sanchez RM, Adzet T, Laguna JC, Carrera MV. Increased reactive oxygen species production down-regulates peroxisome proliferator-activated alpha pathway in C2C12 skeletal muscle cells. J Biol Chem 2002;277:10100–10107.

[22] Kannan R, Jin M, Gamulescu MA, Hinton DR. Ceramide-induced apoptosis: Role of catalase and epatocyte growth factor. Free Radic Biol Med 2004;37:166–175.

[23] Goldkorn T, Ravid T, Khan EM. Life and death decisions: Ceramide generation and EGF receptor trafficking are modulated by oxidative stress. Antioxid Redox Signal 2005;7:119–128.

[24] Lavrentiadou SN, Chen C, Kawcak T, Ravid T, Tsaba A, van der Vliet A, Rasooly R, Goldkorn T. Ceramide-mediated apoptosis in lung epithelial cells is regulated by glutathione. Am J Respir Cell Mol Biol 2001;25:676–684.

[25] Hartman BL, Geley S, Koffler M, Hattmannstorfer R, Strausser-Wozak EM, Auer B, Kofler R. Bcl-2 interferes with the execution phase, but not upstream events, in glucocorticoid-induced leukemia apoptosis. Oncogene 1999;18:713–719.

[26] Triola G, Fabriàs G, Llebaria A. Synthesis of a cyclopropene analogue of ceramide, a potent inhibitor of dihydroceramide desaturase. Angew Chem Int Ed Engl 2001;40:1960–1962.

[27] Bligh EA, Dyer WJ. A rapid method of total lipid extraction and purification. Can J Biochem Physiol 1959;37:911–917.

[28] Jayadev S, Linardic CM, Hannun YA. Identification of arachidonic acid as a mediator of sphingomyelin hydrolysis in response to tumor necrosis factor alpha. J Biol Chem 1994;269:5757–5763.

[29] Boya P, Morales MC, Gonzalez-Polo RA, Andreau K, Goudier I, Perfettini JL, Larochette N, Deniaud A, Baran-Marszak F, Fagard R, Feuillard J, Asumendi A, Raphael M, Pau B, Brenner C, Kroemer G. The chemopreventive agent *N*-(4-hydroxyphenyl)retinamide induces apoptosis through a mitochondrial pahtway regulated by proteins from the Bcl-2 family. Oncogene 2003;22:6220–6230.

[30] Lovat PE, Oliverio S, Corazzari M, Rodolfo C, Ranalli M, Goranov B, Melino G, Redfern CPF, Piancentini M. Bak: A downstream mediator of fenretinide-induced apoptosis of SH-SY5Y neuroblastoma cells. Cancer Res 2003;63:7310–7313.

[31] Morales MC, Pérez-Yarza G, Nieto-Rementería N, Boyano MD, Muhialdin J, Atencia R, Asumendi A. Intracellular glutathione levels determine cell sensitivity to apoptosis induced by the antineoplasic agent *N*-(4-hydroxyphenyl)retinamide. Anticancer Res 2005;25:1945–1952.

[32] Ruffolo SC, Breckenridge DG, Nguyen M, Goping IS, Gross A, Korsmeyer SJ, Li H, Yuan J, Shore GC. BID-dependent and BID-independent pathways for BAX insertion into mitochondria. Cell Death Differ 2000;7:1101–1108.

[33] Kuwana T, Mackey MR, Perkins G, Ellisman MH, Latterich M, Schneiter R, Green DR, Newmeyer DD. Bid, bax, and lipids cooperate to form supramolecular openings in the outer mitochondrial membrane. Cell 2002;111:331–342.

[34] Ahmad KA, Iskandar KB, Hirpara JL, Clement MV, Pervaiz S. Hydrogen peroxide-mediated cytosolic acidification is a signal for mitochondrial translocation of bax during drug-induced apoptosis of tumor cells. Cancer Res 2004;64:7867–7878.

[35] Ott M, Robertson JD, Gogvadze V, Zhivotovsky B, Orrenius S. Cytochrome *c* release from mitochondria proceeds by a two-step process. Proc Natl Acad Sci USA 2002;99:1259–1263.

[36] Nakagawa Y. Initiation of apoptotic signal by the peroxidation of cardiolipin of mitochondria. Ann NY Acad Sci 2004;1011:177–184.

[37] Nomura K, Imai T, Nakagawa Y. Mitochondrial phospholipid hydroperoxide glutathione inhibits the release of cytochome *c* from mitochondria by suppressing the peroxidation of cardiolipin in hypoglycaemia-induced apoptosis. Biochem J 2000;351:183–193.

[38] Reynolds CP, Maurer BJ, Kolesnick RN. Ceramide synthesis and metabolism as a target for cancer therapy. Cancer Lett 2004;206:169–180.

[39] Marchetti P, Zamzami N, Josph B, Schraen-Maschke S, Mereau-Richard C, Costantini P, Metivier D, Susin SA, Kroemer G, Formstecher P. The novel retinoid 6-[3-(1-adamantyl)-4-hydroxyphenyl]-2-naphtalene carboxylic acid can trigger apoptosis through a mitochondrial pathway independent of the nucleus. Cancer Res 1999;54:6257–6275.

[40] Notario B, Zamora M, Vinas O, Mampel T. All-trans-retinoic acid binds to and inhibits adenine nucleotide translocase and induces mitochondrial permeability transition. Mol Pharmacol 2003;63:224–231.

[41] Siskind LJ. Mitochondrial ceramide and the induction of apoptosis. J Bioenerg Biomembr 2005;37:143–153.

[42] García-Ruiz C, Colell A, Mari M, Morales A, Fernandez-Checa JC. Direct effect of ceramide on the mitochondrial electron transport chain leads to generation of reactive oxygen species. Role of mitochondrial glutathione. J Biol Chem 1997;272:11369–11377.

[43] Quillet-Mary A, Jaffrézou JP, Mansat V, Bordier C, Naval J, Laurent G. Implication of mitochondrial hydrogen peroxide generation in ceramide-induced apoptosis. J Biol Chem 1997;272:21388–21395.

[44] Di Paola M, Cocco T, Lorusso M. Ceramide interaction with the respiratory chain of heart mitochondria. Biochemistry 2000;39:6660–6668.

[45] Therade-Mathara S, Laemmel E, Carpentier S, Obata Y, Levade T, Duranteau J, Vicaut E. Reactive oxygen species production by mitchondria in endothelial cells exposed to reoxygenation after hypoxia and glucose depletion is mediated by ceramide. Am J Physiol Regul Integr Comp Physiol 2005;289:1756–1762.

[46] Ghafourifar P, Klein SD, Schucht O, Schenk U, Pruschy M, Rocha S, Richtere C. Ceramide induces cytochrome *c* release from isolated mitochondria. Importance of mitochondrial redox state. J Biol Chem 1999;274:6080–6084.

[47] Di Paola M, Zaccagnino P, Montedoro G, Cocco T, Lorusso M. Ceramide induces release of pro-apoptotic proteins from mitochondria by either a Ca2 + -dependent or a Ca2 + -independent mechanism. J Bioenerg Biomembr 2004;36:165–170.

[48] Schulze-Osthoff L, Bakker AC, Vanhaesebroeck B, Beyaert R, Jacob WA, Fiers W. Cytotoxic activity of tumor necrosis factor is mediated by early damage of mithochondrial functions. Evidence for the involvement of mitochondrial radical generation. J Biol Chem 1992;267: 5317–5323.

[49] Nicolay K, de Kruijff B. Effects of adriamycin on respiratory chain activities in mitochondria from rat liver, rat heart, and bovine heart. Evidence for a preferential inhibition of complex III and IV. Biochim Biophys Acta 1987;892: 320–330.

[50] Tuquet C, Dupont J, Mesneau A, Roussaux J. Effects of tamoxifen on the electron transport chain of isolated rat liver mitochondria. Cell Biol Toxicol 2000;16:207–219.

[51] Chen JSK, Agarwal N, Mehta K. Multigrug-resistant MCF-7 breast cancer cells contain deficient intracellular calcium pools. Breast Cancer Res Treat 2002;71:237–347.

[52] Macho A, Hirsch T, Marzo I, Marchetti P, Dallaporta B, Susin SA, Zamzami N, Kroemer G. Glutathione depletion is an early and calcium elevation is a late event of thymocyte apoptosis. J Immunol 1997;158:4612–4619.

[53] Degterev A, Boyce M, Yuan J. The channel of death. J Cell Biol 2001;155:695–698.

[54] Cheng EH, Wei MC, Weiler S, Flavell RA, Mak TW, Lindsten T, Kornsmeyer SJ. BCL-2 BCL-X(L) sequester BH3 domain-only molecules preventing BAX- and BAK-mediated mitochondrial apoptosis. Mol Cell 2001;8:705–711.